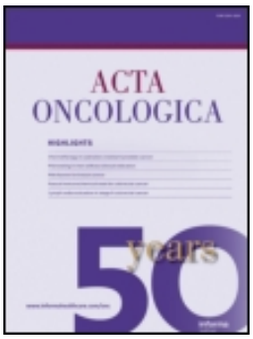

Acta Oncologica

ISSN: 0284-186X (Print) 1651-226X (Online) Journal homepage: informahealthcare.com/journals/ionc20

# Ultra-high field $^{1}$H magnetic resonance imaging approaches for acute hypoxia

Thomas Nielsen, Niels Chr. Nielsen, Thomas H. Holm, Leif Østergaard, Michael R. Horsman & Morten Busk

**To cite this article:** Thomas Nielsen, Niels Chr. Nielsen, Thomas H. Holm, Leif Østergaard, Michael R. Horsman & Morten Busk (2013) Ultra-high field $^{1}$H magnetic resonance imaging approaches for acute hypoxia, Acta Oncologica, 52:7, 1287-1292, DOI: 10.3109/0284186X.2013.824608

**To link to this article:** https://doi.org/10.3109/0284186X.2013.824608

*Acta Oncologica*, 2013; 52: 1287–1292

informa
healthcare

**ORIGINAL ARTICLE**

# Ultra-high field $^{1}$H magnetic resonance imaging approaches for acute hypoxia

THOMAS NIELSEN[1,2], NIELS CHR. NIELSEN[3], THOMAS H. HOLM[4], LEIF ØSTERGAARD[5], MICHAEL R. HORSMAN[1] & MORTEN BUSK[1]

[1]*Department of Experimental Clinical Oncology, Aarhus University Hospital, Aarhus Denmark,* [2]*Interdisciplinary Nanoscience Center (iNANO), Aarhus University, Aarhus, Denmark,* [3]*Center for Insoluble Protein Structures, Interdisciplinary Nanoscience Center (iNANO) and Department of Chemistry, Aarhus University, Aarhus, Denmark,* [4]*Department of Biomedicine, Aarhus University, Aarhus, Denmark and* [5]*Center of Functionally Integrative Neuroscience and MINDLab, NeuroCampus Aarhus, Aarhus University, Aarhus C, Denmark*

**Abstract**

*Background.* Currently, radiation treatments are being optimised based on in vivo imaging of radioresistant, hypoxic tumour areas. This study aimed at detecting nicotinamide's reduction of acute hypoxia in a mouse tumour model by two clinically relevant magnetic resonance imaging (MRI) methods at ultra-high magnetic field strength. *Material and methods.* The C3H mammary carcinoma was grown to 200 mm$^3$ in the right rear foot of CDF$_1$ mice. The mice were anaesthetised with ketamine and xylazine prior to imaging. A treatment group received nicotinamide intraperitoneally (i.p.) at the dose 1000 mg/kg, and a control group received saline. MRI was performed at 16.4 T with a spatial resolution of $0.156 \times 0.156 \times 0.5$ mm$^3$. The imaging protocol included BOLD imaging and two DCE-MRI scans. Initial area under the curve (IAUC) and the parameters from the extended Toft's model were estimated from the DCE-MRI data. Tumour median values of 1) $T_2$* mean, 2) $T_2$* standard deviation, 3) DCE-MRI parameters, and 4) DCE-MRI parameter differences between scans were compared between the treatment groups using Student's t-test (significance level $p < 0.05$). *Results.* Parametric maps showed intra- and inter-tumour heterogeneity. Blood volume was significantly larger in the nicotinamide-treated group, and also the blood volume difference between the two DCE-MRI scans was significantly larger in the treatment group. *Conclusion.* Higher blood volume and blood volume variation was observed by DCE-MRI in the treatment group. Other DCE-MRI parameters showed no significant differences, and the higher blood volume was not detected by BOLD MRI. The higher blood volume variation seen with DCE-MRI may be influenced by the drug effect reducing over time, and furthermore the anaesthesia may play an important role.

Low oxygen levels (hypoxia) exist in solid tumours and are associated with resistance to radiotherapy and poorer outcome after radiotherapy [1,2]. A range of different assays have been utilised to identify hypoxia in different tumour types [3]. Involvement of non-invasive imaging approaches in optimisation of radiotherapy planning is an on-going and active research field [4–7]. Hypoxic markers exist for positron emission tomography (PET), which is characterised by high sensitivity but low spatial resolution compared with computed tomography (CT) and magnetic resonance imaging (MRI). MRI is clinically more available than PET and does not involve ionising radiation. Therefore, there is a desire for MRI-based hypoxia sensitive methods, which may be used for treatment planning and adaptive radiotherapy. The parameters obtained by the perfusion method dynamic contrast-enhanced MRI (DCE-MRI) is currently being investigated in clinical research as indirect information on $pO_2$ or hypoxia [5].

Hypoxia has been divided into two subtypes. In addition to the traditional concept of diffusion-limited chronic hypoxia, acute hypoxia resulting from transient perfusion stoppages has been shown in

Correspondence: T. Nielsen, Interdisciplinary Nanoscience Center (iNANO), The iNANO House, Gustav Wieds Vej 14, Aarhus University, 8000 Aarhus C, Denmark. Tel: +45 87156664. E-mail: thomasn@inano.au.dk.

*(Received 3 July 2013; accepted 9 July 2013)*

ISSN 0284-186X print/ISSN 1651-226X online 
DOI: 10.3109/0284186X.2013.824608

murine tumours [8,9] and observed in different human tumours [10,11]. Different experimental MR methods can assess tumour $pO_2$; these include $^{19}F$ oximetry [12,13], Overhauser MRI (OMRI) [14], and electron paramagnetic resonance imaging (EPRI) [15]. Acute hypoxia has been identified by EPRI [16,17].

Also clinically relevant MRI methods have been suggested for assessing acute hypoxia. Repeated DCE-MRI has been shown to identify regional tumour perfusion changes [18]. Another MRI method, blood oxygenation level dependent (BOLD) MRI, is sensitive to tumour perfusion via changes in deoxyhaemoglobin [19], and fluctuations in the BOLD signal has been suggested as a marker of acute hypoxia [20].

Nicotinamide has been shown to reduce the transient perfusion stoppages responsible for acute hypoxia and thereby provide radiosensitisation in a mouse tumour model, the C3H mammary carcinoma [21,22]. While acute hypoxia has been identified by DCE-MRI and BOLD MRI at clinical and experimental magnetic field strengths, we hypothesised that MRI at ultra-high magnetic field strength would provide not only improved spatial resolution and thereby information on partial volume effects at clinical field strengths, but also a higher sensitivity for the BOLD effect. The aim of this study was to assess acute hypoxia and the effect of nicotinamide by DCE-MRI and BOLD MRI in the C3H mammary carcinoma at ultra-high magnetic field strength.

## Material and methods

### *Drug preparation*

Nicotinamide (Sigma, St. Louis, MO, USA) was prepared fresh before each experiment by dissolving in sterile saline (0.9% NaCl). It was intraperitoneally (i.p.) injected into mice at the dose of 1000 mg/kg at a constant injection volume of 0.02 ml/g body weight. Combined ketamine and xylazine was used for anaesthesia. The stock solutions were dissolved in sterile saline (0.9% NaCl) to a mixture of 10 mg/ml ketamine + 1 mg/ml xylazine, which was administered i.p. at a constant injection volume of 0.01 ml/g body weight for introduction of anaesthesia. A top-up dose of 0.005 ml/g was given for maintenance of anaesthesia every 60 min after the introduction of anaesthesia or earlier if needed based on respiration monitoring.

### *Animal and tumour model*

A C3H mammary carcinoma implanted in the right rear foot of 10–14-week-old female $CDF_1$ mice was used in all experiments. The derivation and maintenance of this tumour have been described previously [23]. Experiments were performed when tumours had reached approximately 200 $mm^3$ in size, which typically occurred three weeks after inoculation. Tumour volume was calculated from the formula $D1 \times D2 \times D3 \times \pi/6$, where the D values represent the three orthogonal diameters. All procedures involving experimental animals were approved by the National Animal Experiments Inspectorate.

### *In vivo MRI*

A 16.4 T Bruker Avance II spectrometer (Bruker BioSpin GmbH, Rheinstetten, Germany) equipped with a gradient system was used for DCE-MRI. Female $CDF_1$ mice (12–20 weeks old) were anesthetised and injected i.p. with either nicotinamide (treatment group, $n = 3$) or saline (control group, $n = 4$). An intravenous (i.v.) line was applied in a tail vein for administration of the contrast agent Gd-DTPA (Magnevist, Schering, Berlin, Germany), and an i.p. line was inserted for administration of top-up anaesthesia. A respiration monitoring pad was placed at the abdomen of the mice and connected to a monitoring system.

The MRI protocol included BOLD MRI followed by repeated DCE-MRI. The total BOLD imaging time was 20 min, and each DCE-MRI scan had duration of 30 min. DCE-MRI scan #1 was initiated shortly following BOLD imaging, and a second DCE-MRI scan was performed about 1 h after the start of the first DCE-MRI scan. The timings of the scan initiations relative to the treatment (mean $\pm$ SE) were for BOLD MRI: $48 \pm 6$ min, for DCE-MRI scan #1: $78 \pm 7$ min, and for DCE-MRI scan #2: $146 \pm 6$ min.

For the BOLD imaging, 9 or 10 contiguous slices were chosen with a central slice through the tumour centre. A multiple gradient echo sequence was used with 12 $T_E$ values for obtaining 10 (for one tumour 4) repeated $T_2$* maps with the spatial resolution $0.5 \times 0.16 \times 0.16$ $mm^3$. When acquiring the DCE-MRI images, a single slice through the centre of the tumour, corresponding with the central slice from the BOLD MRI, was chosen, and the images were acquired with the same spatial resolution as the BOLD images. A variable repetition time (VTR) sequence with six $T_R$ values was used for $T_1$ mapping during 20 min followed by dynamic image acquisition using a fast spoiled gradient echo sequence during 10 min with a time resolution of approximately 6 s for the dynamic images. During the initial 4 s of the sixth image acquisition, Gd-DTPA was administered i.v. at a dose of 0.1 mmol/kg and concentration of 0.02 M.

The image post-processing and statistics was done in Matlab 7.14 (The MathWorks, Inc., Natick, MA, USA). All images were smoothed using a $5 \times 5$ matrix Gaussian filter with standard deviation 1. $T_1$ maps were calculated from the VTR images. We

assumed a linear relationship between Gd-DTPA concentration and $\Delta R_1$ ($R_1 = 1/T_1$), with a relaxivity of 3.04 $(mM \bullet s)^{-1}$ (own data determined for blood plasma at the system, data not shown). Voxel concentration-time curves were used to calculate maps of vascular parameters. The semi-quantitative parameter initial area under the curve (IAUC) was calculated by integration of the Gd-DTPA concentration over the first 90 s post-administration. Voxels with very low IAUC values cannot be used for model analysis, and therefore voxels with IAUC less than 0.5 mM•s were assumed not vascularised and excluded from the DCE-MRI analysis.

The standard DCE-MRI model including a vascular term was fitted to the curves for quantitative estimation of the transfer constant, $K^{trans}$, the rate constant, $k_{ep}$, the extravascular extracellular space, $v_e = K^{trans}/k_{ep}$, and the plasma volume fraction, $v_p$ [24]. Tracer plasma concentration was based on measurements by Furman-Haran et al. [25] and adapted in this experiment with the current dose assuming a blood volume of 65 ml/kg and a haematocrit of 0.49 [26]. Fitting was performed using the trust-region-reflective algorithm with lower bound 0 and no upper bound for all parameters. The criterion for an acceptable fit was a mean fit point distance to the measured points larger than or equal to 0.5 M.

Regions of interest (ROIs) were drawn manually around the tumours on the MR-images. Voxels not satisfying the DCE-MRI model fit criterion were excluded. Tumour median values of 1) $T_2$* mean, 2) $T_2$* standard deviation, 3) DCE-MRI parameters, and 4) DCE-MRI parameter differences between scans were compared between the treatment groups using Student's t-test (significance level $p < 0.05$) for identifying acute hypoxia and the effect of nicotinamide.

## Results

Figure 1 shows maps of $T_2$* mean and SD for the BOLD MRI time interval for a saline treated control tumour. The maps show heterogeneity at this relatively high spatial resolution level. Table I summarises statistics on the median tumour $T_2$* mean and SD. No statistically significant differences between the treatment groups were found. Figure 2 shows DCE-MRI parametric maps for the same control tumour, and these parameters also show heterogeneity at the spatial resolution level. Table II summarises statistics on the median tumour DCE-MRI parameter values. $v_p$ was significantly higher in the nicotinamide-treated group for both the first DCE-MRI scan ($p = 0.0005$) and the second DCE-MRI scan ($p = 0.002$), and also the absolute difference in $v_p$ between the two DCE-MRI scans was significantly higher in the nicotinamide-treated group ($p = 0.04$). All other parameters showed no statistically significant differences between the treatment groups.

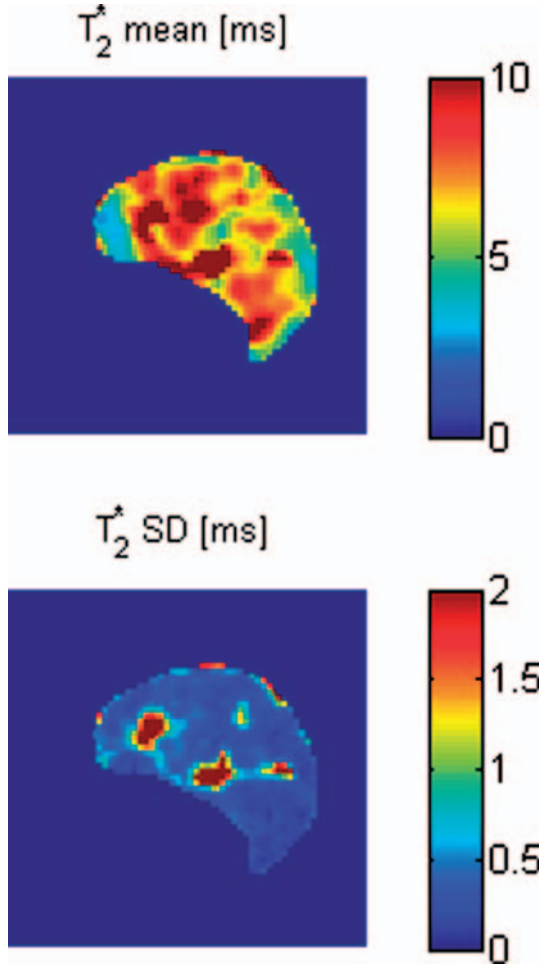


Figure 1. BOLD MRI parametric maps of $T_2$* mean and SD for a control tumour.

## Discussion

The present study aimed at evaluating acute hypoxia and changes induced by nicotinamide using clinically relevant MRI methods at ultra-high magnetic field strength. Neither the mechanism responsible for the intermittend blood flow causing acute hypoxia nor the mechanism by which nicotinamide reduces acute hypoxia is known, but suggestions are summarised in

Table I. BOLD MRI parameter values.

| | $T_2$* mean [ms] | $T_2$* SD [μs] |
|---|---|---|
| **Saline** | 7.50 ± 1.48 | 248 ± 33.8 |
| **Nicotinamide** | 8.74 ± 1.30 | 253 ± 26.6 |

Tumour median values of the $T_2$* mean and SD for the BOLD MRI time interval. Parameter values are shown as mean ± SE of individual tumour medians. The data showed no statistically significant differences between the treatment groups.

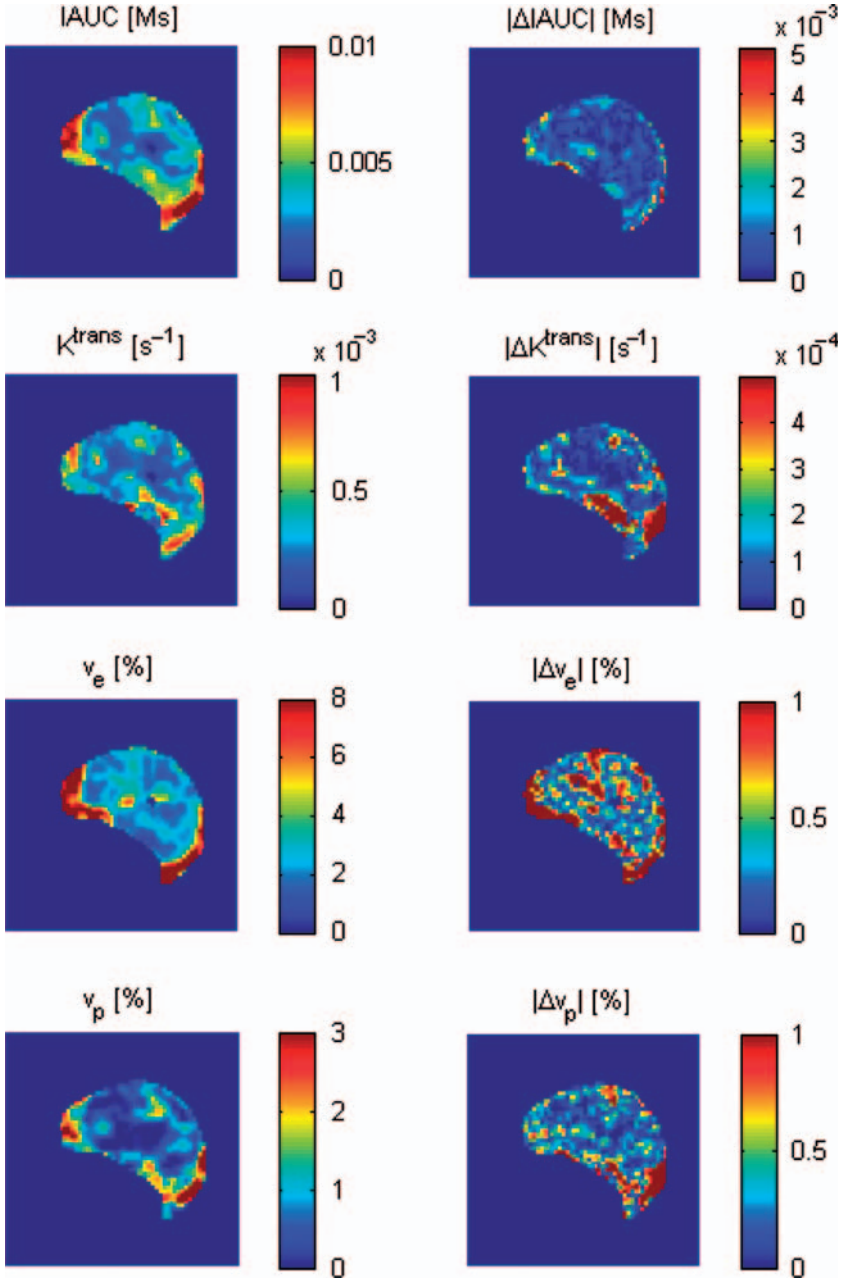


Figure 2. DCE-MRI parametric maps for the same control tumour as shown in Figure 1. Initial maps and difference maps for the two DCE-MRI scans are shown.

a review by Horsman [27]. Suggested causative factors for intermittend blood flow are vessel plugging by blood cells or circulating tumour cells, high interstitial fluid pressure, and spontaneous vasomotor activity in upstream vessels. While there is no evidence that nicotinamide prevents vessel plugging, nicotinamide has been shown to reduce interstitial fluid pressure, and there is preliminary ex vivo evidence for reduction of spontaneous arterial contraction by nicotinamide. Both of these effects were observed at relatively high doses comparable to the dose in the present study, and at such high doses, nicotinamide is also known to reduce mean arterial blood pressure, which may explain the reduction in interstitial fluid pressure. Radiosensitisation is however present at lower doses not affecting the blood pressure, but it is not known whether these doses affect interstitial fluid pressure.

The used pharmacokinetic DCE-MRI model was extended from the standard model to estimate the fractional blood plasma volume $v_p$, which is otherwise assumed to be zero. This was the only parameter showing statistically significant differences between the treatment groups in this study.

Table II. DCE-MRI parameter values.

| A | IAUC [mM*s] | $K^{trans}$ [$\mu s^{-1}$] | $v_e$ [%] | $v_p$ [‰] |
|---|---|---|---|---|
| **Saline** | 3.90 ± 0.804 | 545 ± 132 | 3.59 ± 0.409 | 1.19 ± 0.653 |
| **Nicotinamide** | 4.53 ± 0.327 | 342 ± 74.9 | 3.26 ± 0.256 | 8.71 ± 0.510* |
| **B** | **IAUC [mM*s]** | **$K^{trans}$ [$\mu s^{-1}$]** | **$v_e$ [%]** | **$v_p$ [‰]** |
| **Saline** | 4.43 ± 0.509 | 594 ± 121 | 3.69 ± 0.323 | 1.20 ± 0.360 |
| **Nicotinamide** | 4.77 ± 0.452 | 514 ± 160 | 3.08 ± 0.380 | 5.23 ± 0.634* |
| **C** | **\|ΔIAUC\| [mM*s]** | **\|$\Delta K^{trans}$\| [$\mu s^{-1}$]** | **\|$\Delta v_e$\| [‰]** | **\|$\Delta v_p$\| [‰]** |
| **Saline** | 1.01 ± 0.540 | 161 ± 29.6 | 6.82 ± 0.906 | 1.72 ± 0.317 |
| **Nicotinamide** | 0.680 ± 0.0440 | 165 ± 61.2 | 6.44 ± 0.611 | 3.06 ± 0.401* |

Parameter values are shown as mean ± SE of individual tumour medians. A. Initial DCE-MRI values. B. DCE-MRI values for the second DCE-MRI scan. C. Absolute difference values between the two DCE-MRI scans. An asterisk (*) indicates for the nicotinamide group a statistically significant difference from the saline group.

The main result was a significantly higher $v_p$ in the nicotinamide-treated group, which was intuitively expected because that nicotinamide has been shown to prevent the vessel collapses responsible for acute hypoxia. This is, however, not in agreement with our data from a previous study, where the effect of nicotinamide on DCE-MRI parameters appeared in the extravascular extracellular space $v_e$ [28]. This change in $v_e$ likely related to the known effect of nicotinamide on interstitial fluid pressure. A number of factors differed between these studies, and this may explain the different results. The current study was carried out at ultra-high magnetic field strength with the mice being anaesthetised in a vertical position, where the previous study was carried out in a 3T clinical magnet with the mice unanaesthetised in a prone position. Therefore, the circulation physiology may have differed; including systematic deviations from the population-based arterial input function used in the DCE-MRI model analysis.

Nicotinamide induced a significantly larger blood volume $v_p$ but no significant changes in $K^{trans}$, which relates to perfusion and permeability. A cautious interpretation of these results was that the larger percentage of open vessels caused by nicotinamide resulted in a perfusion redistribution rather than a perfusion increase. An unexpected result was the larger variation in DCE-MRI assessed functional blood volume in the nicotinamide-treated tumours. A possible explanation is that nicotinamide has a peak effect at about 1 h, and this effect is reduced at longer time intervals [21,29]. The time from drug or saline treatment to the end of the second DCE-MRI scan ranged from about 2 1/2–3 1/2 h, and therefore, the drug effect might have been systematically reduced at the time of the second DCE-MRI scan compared with the first DCE-MRI scan. This is in agreement with the lower $v_p$ value estimated from the second DCE-MRI scan compared with the value estimated from the first DCE-MRI scan.

The BOLD imaging did not show different $T_2$* mean or standard deviation over 20 min. The standard deviation approach for assessing acute hypoxia was rather simplistic. More exploratory statistics on $T_2$*-weighted images and $T_2$* maps was applied by Baudelet et al. [20], and they found most perfusion cycling in the low-frequency-band with less than one cycle per 3 min. Our BOLD imaging frame rate should be sensitive to this frequency level, and we expected our experimental setting to be highly sensitive to acute hypoxia due to the susceptibility effect sensitivity and spatial resolution. Still, we found no difference in $T_2$* standard deviation between the treatment groups despite the different fractional blood volumes. We would also have expected these different fractional blood volumes to cause a difference in the mean $T_2$* because of different levels of deoxyhaemoglobin.

## Conclusions

Using the clinically feasible perfusion methods BOLD MRI and DCE-MRI at ultra-high magnetic field strength for assessing acute hypoxia, we were able to detect higher fractional blood volume induced by nicotinamide and higher blood volume variation in in this treatment group. Other DCE-MRI parameters showed no significant differences, and the higher blood volume induced by nicotinamide was not detected by BOLD MRI. The higher blood volume variation seen with DCE-MRI may be influenced by the drug effect reducing over time, and furthermore the anaesthesia may play an important role when investigating circulation-related imaging parameters preclinically.

## Acknowledgements

The authors would like to thank Inger Marie Horsman, Dorthe Grand, Pia Schjerbeck, Kristina Lystlund Lauridsen, and Mogens Jøns Johannsen for excellent technical assistance.

***Declaration of interest:*** The authors report no conflicts of interest. The authors alone are responsible for the content and writing of the paper.

This work has been funded with support from The Danish Cancer Society, the METOXIA project no. 222741 under the 7th Research Framework Programme of the European Union, the Danish National Research Foundation (DNRF59), CIRRO – the Lundbeck Foundation Center for Interventional Research in Radiation Oncology, and the Danish Council for Strategic Research.

## References

[1] Nordsmark M, Overgaard M, Overgaard J. Pretreatment oxygenation predicts radiation response in advanced squamous cell carcinoma of the head and neck. Radiother Oncol 1996; 41:31–9.

[2] Overgaard J. Hypoxic modification of radiotherapy in squamous cell carcinoma of the head and neck – a systematic review and meta-analysis. Radiother Oncol 2011;100:22–32.

[3] Overgaard J. Hypoxic radiosensitization: Adored and ignored. J Clin Oncol 2007;25:4066–74.

[4] Mortensen LS, Johansen J, Kallehauge J, Primdahl H, Busk M, Lassen P, et al. FAZA PET/CT hypoxia imaging in patients with squamous cell carcinoma of the head and neck treated with radiotherapy: Results from the DAHANCA 24 trial. Radiother Oncol 2012;105:14–20.

[5] Horsman MR, Mortensen LS, Petersen JB, Busk M, Overgaard J. Imaging hypoxia to improve radiotherapy outcome. Nat Rev Clin Oncol 2012;9:674–87.

[6] Tran LB, Bol A, Labar D, Jordan B, Magat J, Mignion L, et al. Hypoxia imaging with the nitroimidazole 18F-FAZA PET tracer: A comparison with OxyLite, EPR oximetry and 19F-MRI relaxometry. Radiother Oncol 2012;105: 29–35.

[7] Gulliksrud K, Ovrebo KM, Mathiesen B, Rofstad EK. Differentiation between hypoxic and non-hypoxic experimental tumors by dynamic contrast-enhanced magnetic resonance imaging. Radiother Oncol 2011;98:360–4.

[8] Brown JM. Evidence for acutely hypoxic cells in mouse tumours, and a possible mechanism of reoxygenation. Br J Radiol 1979;52:650–6.

[9] Chaplin DJ, Durand RE, Olive PL. Acute hypoxia in tumors: Implications for modifiers of radiation effects. Int J Radiat Oncol Biol Phys 1986;12:1279–82.

[10] Powell ME, Hill SA, Saunders MI, Hoskin PJ, Chaplin DJ. Human tumor blood flow is enhanced by nicotinamide and carbogen breathing. Cancer Res 1997;57:5261–4.

[11] Begg AC, Janssen H, Sprong D, Hofland I, Blommestijn G, Raleigh JA, et al. Hypoxia and perfusion measurements in human tumors – initial experience with pimonidazole and IUdR. Acta Oncol 2001;40:924–8.

[12] Mason RP, Rodbumrung W, Antich PP. Hexafluorobenzene: A sensitive 19F NMR indicator of tumor oxygenation. NMR Biomed 1996;9:125–34.

[13] Le D, Mason RP, Hunjan S, Constantinescu A, Barker BR, Antich PP. Regional tumor oxygen dynamics: 19F PBSR EPI of hexafluorobenzene. Magn Reson Imaging 1997;15:971–81.

[14] Krishna MC, English S, Yamada K, Yoo J, Murugesan R, Devasahayam N, et al. Overhauser enhanced magnetic resonance imaging for tumor oximetry: Coregistration of tumor anatomy and tissue oxygen concentration. Proc Natl Acad Sci U S A. 2002;99:2216–21.

[15] Matsumoto K, Subramanian S, Devasahayam N, Aravalluvan T, Murugesan R, Cook JA, et al. Electron paramagnetic resonance imaging of tumor hypoxia: Enhanced spatial and temporal resolution for in vivo pO2 determination. Magn Reson Med 2006;55:1157–63.

[16] Yasui H, Matsumoto S, Devasahayam N, Munasinghe JP, Choudhuri R, Saito K, et al. Low-field magnetic resonance imaging to visualize chronic and cycling hypoxia in tumor-bearing mice. Cancer Res 2010;70:6427–36.

[17] Matsumoto S, Yasui H, Mitchell JB, Krishna MC. Imaging cycling tumor hypoxia. Cancer Res 2010;70:10019–23.

[18] Brurberg KG, Benjaminsen IC, Dorum LM, Rofstad EK. Fluctuations in tumor blood perfusion assessed by dynamic contrast-enhanced MRI. Magn Reson Med 2007;58: 473–81.

[19] Robinson SP, McIntyre DJO, Checkley D, Howe JJTaFA, Griffiths JR, Ashton SE, et al. Tumour dose response to the antivascular agent ZD6126 assessed by magnetic resonance imaging. Br J Cancer 2003;88:1592–7.

[20] Baudelet C, Ansiaux R, Jordan BF, Havaux X, Macq B, Gallez B. Physiological noise in murine solid tumours using T2*-weighted gradient-echo imaging: A marker of tumour acute hypoxia? Phys Med Biol 2004;49:3389–411.

[21] Horsman MR, Chaplin DJ, Overgaard J. Combination of nicotinamide and hyperthermia to eliminate radioresistant chronically and acutely hypoxic tumor cells. Cancer Res 1990;50:7430–6.

[22] Horsman MR, Nordsmark M, Khalil AA, Hill SA, Chaplin DJ, Siemann DW, et al. Reducing acute and chronic hypoxia in tumours by combining nicotinamide with carbogen breathing. Acta Oncol 1994;33:371–6.

[23] Overgaard J. Simultaneous and sequential hyperthermia and radiation treatment of an experimental tumor and its surrounding normal tissue in vivo. Int J Radiat Oncol Biol Phys 1980;6:1507–17.

[24] Tofts PS, Brix G, Buckley DL, Evelhoch JL, Henderson E, Knopp MV, et al. Estimating kinetic parameters from dynamic contrast-enhanced T(1)-weighted MRI of a diffusable tracer: Standardized quantities and symbols. J Magn Reson Imaging 1999;10:223–32.

[25] Furman-Haran E, Grobgeld D, Degani H. Dynamic contrast-enhanced imaging and analysis at high spatial resolution of MCF7 human breast tumors. J Magn Reson 1997;128:161–71.

[26] Horsman MR, Finch A, Overgaard J. Erythropoietin improves the oxygen carrying capacity of mouse blood without changing hypoxia in a murine tumour model. Eur J Cancer Suppl 2003;1:S13.

[27] Horsman MR. Nicotinamide and other benzamide analogs as agents for overcoming hypoxic cell radiation resistance in tumours. A review. Acta Oncol 1995;34:571–87.

[28] Horsman MR, Busk M, Nielsen T, Nordsmark M, Overgaard J. Clinical imaging of hypoxia. In: Melillo G, editor. Hypoxia and cancer: Biological implications and therapeutic opportunities. Springer: New York (in press).

[29] Horsman MR, Wood PJ, Chaplin DJ, Brown JM, Overgaard J. The potentiation of radiation damage by nicotinamide in the SCCVII tumour in vivo. Radiother Oncol 1990;18:49–57.